Improvements in the Motion Accuracy of Linear Switched Reluctance Motors

Antares San-Chin Kwok, Wai-Chuen Gan and Norbert C. Cheung

Abstract - **During the last decade, the Linear Switched Reluctance Motor (LSRM) has become popular due to its structural simplicity, robustness and high power density. However, its significant torque ripple creates difficulty on precision motion control. This paper aims to develop a robust control system to improve the motion accuracy of LSRMs.**
The LSRM prototype is firstly investigated to study its force and current relationship. With the help of software, LSRM motion tests are simulated before real experiment. The significant improvement on position control strongly proves the success of the proposal. After that, the experimental result applying on the real prototype closely matches the simulation result.
In order to enhance the LSRM robustness and the position tracking responses, another fuzzy logic controller is newly designed and implemented to supervise the traditional Proportional-Differential (PD) control parameters. Combining the inner control loop on current force relationship and the outer control loop on PD parameter supervision, the LSRM system in this project is very robust and capable to provide a high precision motion performance.

I. Introduction

LSRM has become popular in motor industry during the last decade. Its usage is highlighted with its characteristics such as structural simplicity, robustness, high power density, low cost and promising flexibility in high temperature environment. At the same time, since no magnet is installed, the motor reliability can be improved. In this project, a high performance LSRM is developed based on switched reluctance actuator technology [1, 4]. The translator is supported by 4 pieces of linear motion guide to perform better direct drive motion as improving air gaps.

With the development of the power electronics and the research of various control algorithms, more recent literatures have been shown on reluctance motors application. However, seldom of them provide direct solution on the motion control of short distance and precise specifications. In [6], a several meters long prototype LSRM is designed from a RSRM. While the configuration consists of active stator and passive translator, windings cannot be used effectively and some coils are idol if the translator does not move over them. In [7], the application focuses on the torque control. Only the current control as well as the speed control is performed.

The motion control on LSRM is difficult due to its significant torque ripple resulting from friction uncertainty and flux nonlinearity. Base on reluctance motors characteristics and uneven air gaps, flux linkage cannot be represented as a linear function along the track. This excessive torque ripple causes undesired effect and make noisy on sliding and rotating assemblies. Generally, compensation methods are applied by using a friction model to eliminate the nonlinear friction force. In [8.], despite the model-base method can improve the performance, the control is not robust enough and depends on the parameter accuracy. At the same time, a complicated model analysis and mathematical equation are required for friction compensation.

In this paper, a fuzzy logic control strategy is applied to replace the conventional used numerical approach on handling model nonlinearity problem. Similarly, fuzzy controllers are developed in [9], [10] & [11] but only the simulations results are provided. In this project, the proposed control algorithm would be verified by both simulation and experimental data. The first part of the paper is to develop a table look-up fuzzification to shorten the real time computation time and simplify the control plant. In order to enhance the LSRM robustness and the position tracking responses, another fuzzy logic controller is newly designed and implemented to supervise the traditional PD control parameters in the second part of the paper.

The organization of this paper is as follows. The motor specifications and motion profiles are specified in Section II. Section III presents the fuzzy control system. The table lookup fuzzification is introduced to replace the conventional numerical approach and PID control method. In Section IV, simulation and experimental results are summarized to verify the proposed controller. Finally, the conclusion of the project is given in Section V.

II. Motor Specifications

A. Design schematic

A three-phase coil arrangement with flux de-coupled path and 120 electrical degree separations is shown in the Fig. 1. They are separated with 1+2/3 pitch distance (i.e. X2=10mm). As a result, the pitch distance is designed with 12mm so as to avoid any rounding error from the division by three.

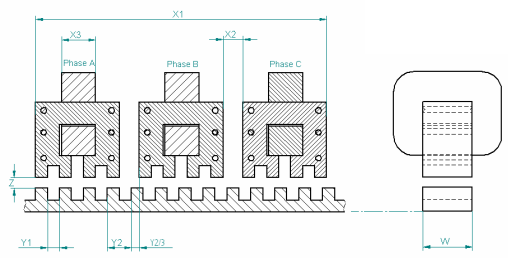

Fig. 1: LSRM design schematic.

The detailed mechanical dimensions and electrical properties of the LSRM prototype are listed in Table. 1.

Power Output	100 W

Antares San-Chin Kwok and Wai-Chuen Gan are with the ASM Assembly Automation Hong Kong Ltd., Kwai Chung, NT, Hong Kong SAR, China (email: {sckwok, wcgan}@asmpt.com).
Norbert C. Cheung is with the Department of Electrical Engineering, The Hong Kong Polytechnic University, Hung Hom, Kowloon, Hong Kong SAR, China. (email: eencheun@polyu.edu.hk).

978-1-4244-1819-0/08/$25.00©2008 IEEE

Maximum Traveling Distance (x)	110 mm
Moving Mass (M)	1.4 kg
Position Accuracy	±25 um
Feedback Device	Optical Encoder with 0.5 um resolution
Pole Width (y_1)	6 mm
Pole Pitch (y_2)	12 mm
Coil Separation (x_2)	10 mm
Winding Width (x_3)	25 mm
Air Gap (z)	0.4 mm
Number of turns per phase (N)	200
Aligned inductance	34mH
Unaligned inductance.	26mH

Table 1: LSRM characteristics.

B. LSRM mathematical model

The switched reluctance linear drive system has a highly non-linear characteristic due to its non-linear flux behavior. Equation (1)-(3) present the general mathematical models of the LSRM:

$$v_j(t) = R_j i_j(t) + \frac{\partial \lambda_j(x(t), i_j(t))}{\partial x(t)} \frac{dx(t)}{dt} + \frac{\partial \lambda_j(x(t), i_j(t))}{\partial i_j(t)} \frac{di_j(t)}{dt} \quad (1)$$

$$j = a, b, c$$

$$f_e = \sum_{j=1}^{3} \frac{\partial \int_0^{i_j(t)} \lambda_j(x(t), i_j(t)) di_j(t)}{\partial x(t)} \quad (2)$$

$$f_e = M \frac{d^2 x(t)}{dt^2} + b \frac{dx(t)}{dt} + f_l(t) \quad (3)$$

where
$v_j(t)$ is the phase voltage,
$i_j(t)$ is the phase current,
$R_j(t)$ is the phase resistance,
λ_j is the phase flux linkage,
x is the travel distance,
f_e is the generated electromechanical force,
f_l is the external load force,
M is the mass and
b is the frictional constant.

C. Motion profiles

For precise motion control, a position tracking profile is usually prepared for position feedback control during the whole traveling motion rather than to control the endpoint accuracy. A 3rd order position S-profile with a limited input bandwidth is a typical practice to eliminate the sudden disturbance to the motor. Equation (4)–(6) govern the 3rd order S-profile generation:

$$\frac{da(t)}{dt} = \{J_{\max}, 0, -J_{\max}\} \quad (4)$$

$$v(t) = \int a(t) dt \quad (5)$$

$$s(t) = \int v(t) dt \quad (6)$$

where a(t) is acceleration, v(t) is velocity and s(t) is position

To verify that the prototype motor is suitable for general pick and place robotic applications in semiconductor industry, 100mm motion profile is described in Fig. 2-4 and 250um motion profile is described in Fig. 5-7. For 100mm long distance profile, maximum acceleration is $4ms^{-2}$ and maximum velocity is $0.48ms^{-1}$. The profile time is 1100ms. For 250um long distance profile, maximum acceleration is $0.8ms^{-2}$ and maximum velocity is $0.01ms^{-1}$. The profile time is 200ms only.

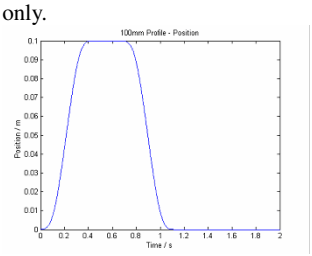

Fig. 2: Position profile of 100mm long distance.

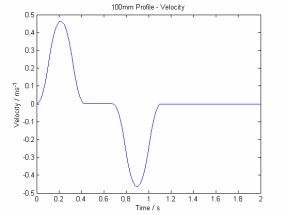

Fig. 3: Velocity profile of 100mm long distance.

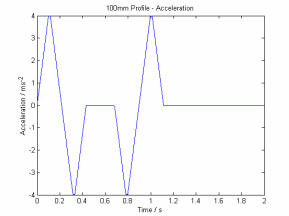

Fig. 4: Acceleration profile of 100mm long distance.

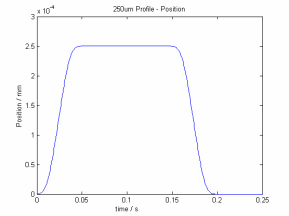

Fig. 5: Position profile of 250um long distance.

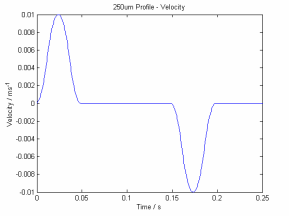

Fig. 6: Velocity profile of 250um long distance.

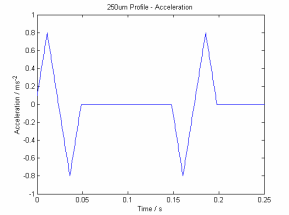

Fig. 7: Acceleration profile of 250um long distance.

III. CONTROL SYSTEM

A. Conventional controller and fuzzy logic controller comparisons

A typical conventional controller is shown in the Fig. 8.

The controller starts with a mathematical model of the plant or process. Theoretically, the relationship between control parameter and process result is assumed to be linear or follow a set of derived differential equations. A number of mathematical derivation and physical prove are necessary. Fig. 9 describes a more intelligent controller, fuzzy logic controller which controls human behavior under certain conditions. This controller needs not a deep understanding of the plant or process. Complicated mathematical model and sophisticated linear/nonlinear control theory can be saved. It implies the logical model of the thinking process used in a human operator during manipulation. Both controller characteristics are summarized in Table. 2.

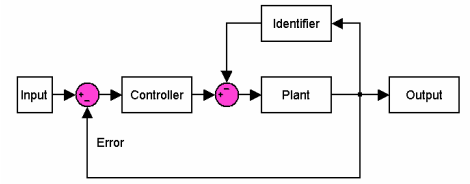

Fig. 8: The conventional controller.

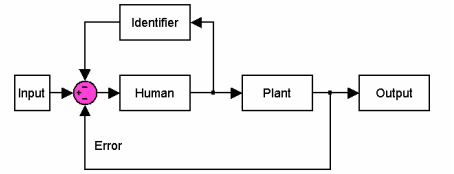

Fig. 9: Fuzzy logic controller.

Conventional controller
1. Identify the plant or process
2. Start with mathematical models
3. Assume defined relationship between control parameter and process result
Fuzzy logic controller
1. Identify the human behavior
2. Start with human expertise
3. No assumption

Table 2: Conventional and fuzzy logic controller comparisons.

B. Table look-up fuzzification

In the fuzzy system applied in the LSRM controller, the fuzzification and defuzzification require a real time computing on membership function equations. To shorten computation time, a table look-up fuzzification technique is investigated. In [13], the table look-up representation of the fuzzy rule base is applied and observed that the final control performance is indistinguishable from that of the pure neural network controller and even provide more successful result in some cases.

The table look-up scheme involves five steps to design the fuzzy system:

Step 1

Normalize input and output valves on their whole possible range.

Step 2

Pre-calculate the membership valves from 0 to 1 to generate rules from input-output pairs. Fig. 10 shows the different membership valves for two-inputs and one-output case. From the pair $(x_{01}^1, x_{02}^1, y_0^1)$, the IF-THEN rule should be : *IF x1 is B1 and x2 is S1, THEN y is CE.* Shown in Fig.10, *S3, S2, S1, CE, B1, B2, B3* are triangular fuzzifiers to represent membership function.

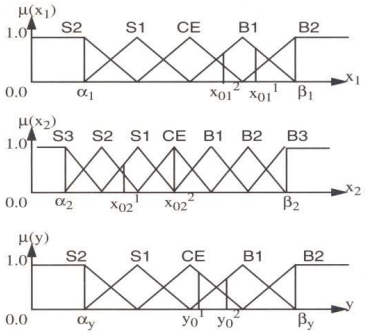

Fig. 10: Membership functions of input-output pairs.

Step 3

Assign a degree to each rule generated from the input-output pair in Step 2 based on the following equation.

$$D(rule) = \mu_{B1}(x_{01}^1)\mu_{S1}(x_{02}^1)\mu_{CE}(y_0^1) \qquad (7)$$

Step 4

Create fuzzy rule base by inserting the fuzzy set into discrete look-up table cells which represent input and output valve relationships shown in Fig.10. Fig. 11 is the example of look-up table.

X_2 \ X_1	S2	S1	CE	B1	B2
S3	S2	S3			
S2	S2	S3	S3	S3	
S1	B1	S1	S2	S3	S2
CE	B2	B2	CE	S2	S2
B1	B2	B3	B2	B1	S1
B2		B3	B3	B3	B2
B3				B3	B2

Fig. 11: Table look-up illustration of the fuzzy rule base.

Step 5

Apply interpolations shown in Fig. 12 for those input valves between the discrete cells. Instead of fuzzifying the discrete variables on line, the fuzzified values are proposed to be looked up by interpolating between the discrete values if the input values fall outside the grid.

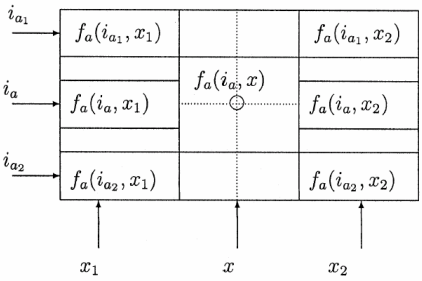

Fig. 12: Interpolating f_a from fuzzified table.

For the inputs $f_a(i_{a_1}, x_1), f_a(i_{a_2}, x_2), f_a(i_{a_1}, x_2), f_a(i_{a_2}, x_2)$ where $i_{a_1} \le i_a \le i_{a_2}$ and $x_1 \le x(t) \le x_2$, the two intermediate values can be found using following equations.

$$f_a(i_a(t),x_1) = f_a(i_a(t),x_1) + \left(\frac{i_a(t)-i_{a_1}}{i_{a_2}-i_{a_1}}\right)[f_a(i_{a_2},x_1) - f_a(i_{a_2},x_1)] \quad (8)$$

$$f_a(i_a(t),x_2) = f_a(i_a(t),x_2) + \left(\frac{i_a(t)-i_{a_1}}{i_{a_2}-i_{a_1}}\right)[f_a(i_{a_2},x_2) - f_a(i_{a_2},x_2)] \quad (9)$$

Finally, the output force value can be computed by

$$f_a(i_a(t),x(t)) = f_a(i_a(t),x_1) + \left(\frac{x(t)-x_1}{x_2-x_1}\right)[f_a(i_a,x_2) - f_a(i_a,x_1)] \quad (10)$$

Since fuzzy rule calculation is done offline, only interpolation is applied in real time operation to replace complicated fuzzification and defuzzification computation. Process time is shortened to achieve faster response. At the same time, table construction approach is much simpler than maintaining a number of fuzzy rules. From the view of investment, the hardware cost is reduced due to less demanding on high speed real time processing. Consequently, table look-up fuzzification is economic and the approach is highly proposed.

Kd is the derivative gain to improve the stability of the system by increasing the damping.

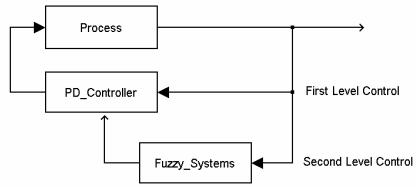

Fig. 13: Fuzzy supervising PD controller.

For a fast response and accurate robot application, the robot arm would not stay at the end point for long time and the static error is very small. Majority of the position error accumulate from dynamic error. Therefore, *Ki* is not considered in feedback control. Unfortunately, PD controllers work under the assumption of linear error functions. If the process input-output relationship is nonlinear, periodic tuning of the controller parameter is required. Therefore, fuzzy control is proposed to take a role to supervise PD gain parameters instead of fine tune the parameters periodically. Fig. 13 shows the proposed controller architecture. The first level is PD controller and

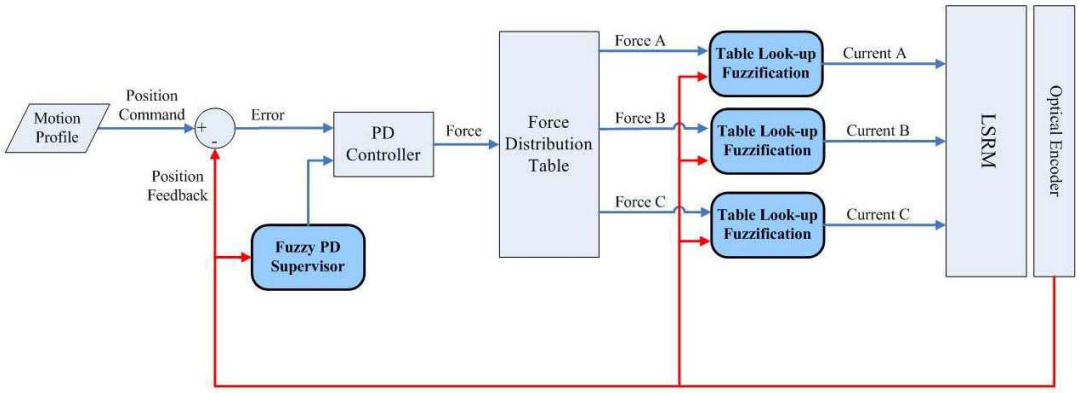

Fig. 14: The proposed controller of the whole LSRM system.

C. Fuzzy logic PD supervisory controller

In a complex practical system, single loop control systems may not effectively achieve the control objectives but a multi level control structure turns out to be very helpful. In this project, the multi level controller is proposed. The lower level controller performs fast direct control and the higher level controller performs low speed supervision. In industry, the majority of robotic feedback controllers are using Proportional-Integral- Differential (PID) controllers. Depends on the process or plant behavior required, PID controllers determine the best mutual adjustment of fixed weighing constants

$$i = Kp * x + Kd * \frac{dx}{dt} + Ki * \int x dt \quad (11)$$

where

Kp is the proportional gain to improve the sensitivity to parameter variations.

Ki is the integral gain to improve the steady-state accuracy.

the second level fuzzy system adjusts the PD parameters according to certain heuristic rules. In this supervisory controller, the profile distance is the input variable while the position gain and the velocity gain are the output variables.

D. The proposed controller of the whole LSRM system

Applying the table look-up fuzzification in the inner control loop to represent the force and current relationship and supervising the feedback parameters (position gain and velocity gain) in the outer position loop by fuzzy logic controller, the integrated controller for the whole LSRM system is proposed in Fig. 14. Comparing with the conventional numerical controller, the real-time processing can be improved and the motor becomes more robust over a wide range of traveling applications.

IV. RESULTS

A. Experimental setup

In this project, in order to implement the proposed control algorithm on LSRM, dSPACE is selected as the hardware interface between the host Personal Computer (PC) and the controller. Apart from hardware, software used includes Matlab/Simulink and ControlDesk. The whole LSRM control diagram is shown in Fig. 15.

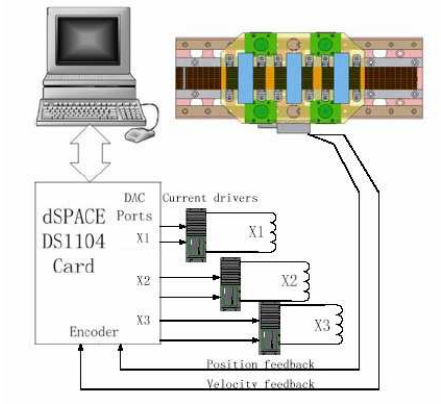

Fig. 15: The diagram of dSPACE controller

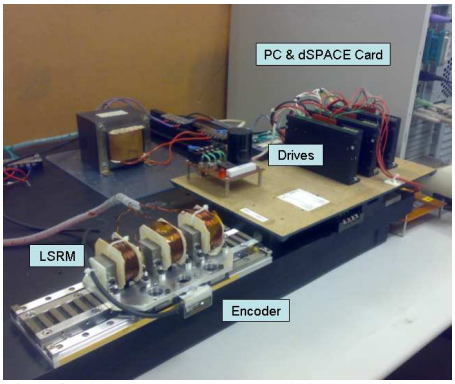

Fig. 16: The LSRM prototype and the control hardware setup in the laboratory

With the use of Simulink software, the motion control program is initially written for simulation which could only provide the theoretical result. Therefore, a series of experiments will be taken to evaluate the simulation results and proposed control algorithm.

Before motion tests, the program is firstly complied and saved in dSPACE card for real time computing. During experiments, ControlDesk software controls online parameter settings and collects instantaneous motor data such as position, velocity, acceleration and current applied. At the same time, the dSPACE card hardware provides computed output voltages to control motion drives to provide exciting current for coil windings. Then, the measured translator position error can be used to compare different control algorithms.

As shown in Fig. 16, a Pentium IV personal computer is used with a dSPACE DS1104 card for program compiling and motion control in real time operation. To provide motor power, three PWM drivers with DC voltage supply 150V is employed to vary input current for three different coils. A Renishaw encoder (RGH24Z) with 0.5um resolution is used as the translator position sensing device. During operation, the position feedback controller applies the sampling frequency in 2kHz which covers most of the significant mechanical vibrations.

B. Calculation of control parameters

Since LSRM is usually applied on continuous series motions, very short settling time is expected and the integral component can be ignored. The whole LSRM position controller can be simplified to be a closed loop control system with PD gain only and presented in Fig. 17.

By employing transfer function, the outer loop control parameter K_P and K_D can be calculated with the frictional characteristics of the motor. These frictional parameters can be measured from the real model and the valves are found as below.

1) Static friction = 0.5N
2) Frictional constant, b = 0.4kg/ms^{-1}
3) Average motor force constant, K_m = 4N/A.

By employing transfer function, the outer loop control parameter K_P and K_D can be calculated with the frictional characteristics of the motor. These frictional

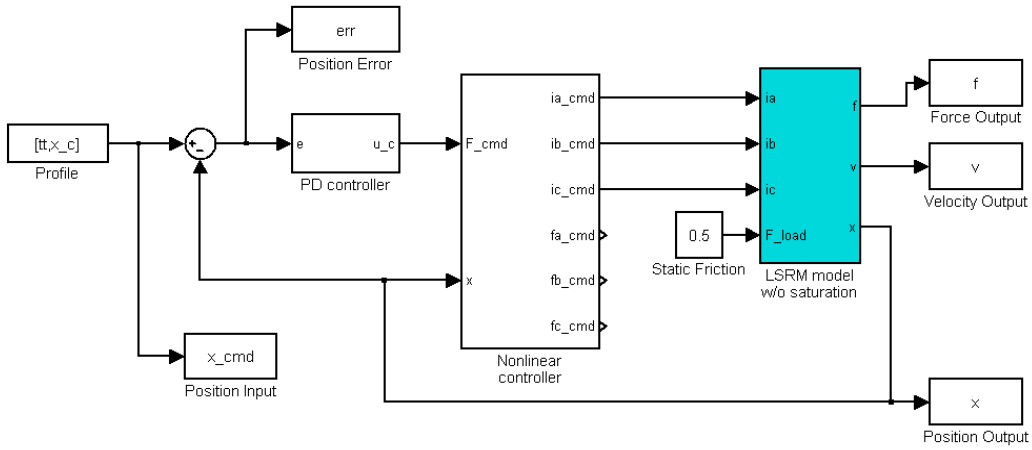

Fig. 17: LSRM simulation diagram using the actual force measurement

parameters can be measured from the real model and the valves are found as below.

For a PD feedback controller,

$$G_C = K_P + K_D s \tag{12}$$

To simplify the calculation, LSRM is assumed to be 2nd order function.

$$G = \frac{K_m}{s(Ms+b)} \tag{13}$$

$$G = \frac{4}{s(1.4s+0.4)}$$

Transfer function = Actual position / Desired position

$$T(s) = \frac{G_C G}{1+G_C G} \tag{14}$$

$$T(s) = \frac{2.6K_D s + 2.6K_P}{s^2 + (K_D + 0.007)2.6s + 2.6K_P}$$

The deadbeat system approach is employed to solve the transfer function. Settling time, T_s is set to be 25ms. Constant, ω_n is 193. Based on 2nd order function,

$$T(s) = \frac{\omega_n^2}{s^2 + 1.82\omega_n s + \omega_n^2} \tag{15}$$

$$s^2 + 351s + 37249 = 0 \tag{16}$$

$$K_P = 14200$$

$$K_D = 135$$

C. Proposed current force controller

Before comparing the performance of the conventional numerical controller and the proposed controller, simulations are done with two different controllers individually to verify the result shortly. The simulation framework is shown is Fig. 17 and LSRM model blue box will use the previously measured force distribution in the real LSRM.

For the numerical approach in the force-current controller, it is assumed that the force output is proportional to the square of exciting current. The magnetic force changes at different positions and thus a sine function is used to represent the force behavior along the motor teeth. The force distribution is shown in the following figures.

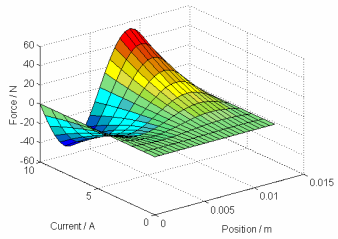

Fig. 18: 3D curve of theoretical force against position and current.

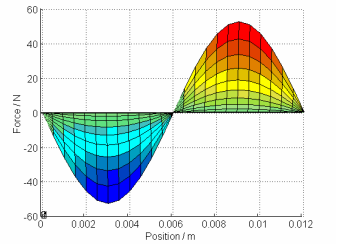

Fig. 19: Theoretical force against position.

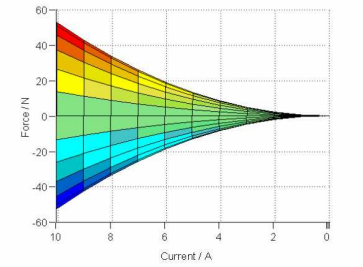

Fig. 20: Theoretical force against current.

From the measurement result in Fig. 21-23, the force output is only proportional to the square of current until the current is under than 2A. In case that the current is higher than 4A, the force output becomes linearly proportional to the current valve. The theoretical assumption is applicable for exciting current lower than 2A. In the proposed fuzzy controller, the current output is adjusted to follow linear proportional relationship when current is high.

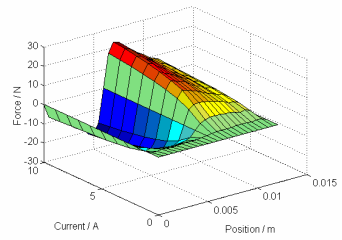

Fig. 21: 3D curve of actual force against position and current.

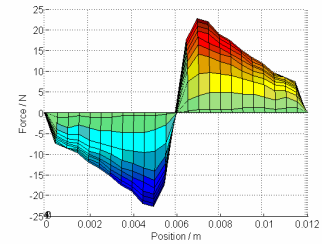

Fig. 22: Actual force against position.

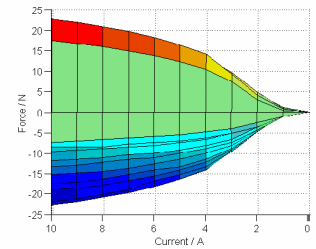

Fig. 23: Actual force against current.

Along the motor teeth axis, asymmetrical force distribution is discovered. This phenomenon is caused by the end effect of the motor teeth corner. Since the partial magnetic flux escapes at the laminated metal plate corner, the magnetic field and hence the generated force become weaker. In the proposed fuzzification lookup table controller, higher current will be given to compensate the magnetic flux loss. Similar to the theoretical force distribution, the proposed force current controller is

presented in Fig. 24-26.

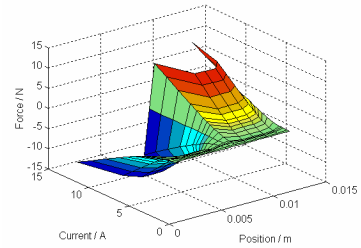

Fig. 24: 3D curve of force against position and current in the proposed controller.

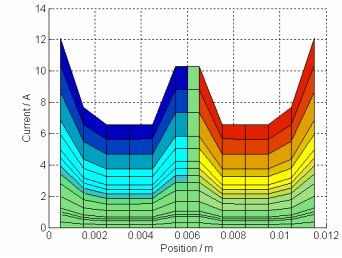

Fig. 25: Force against position in the proposed controller.

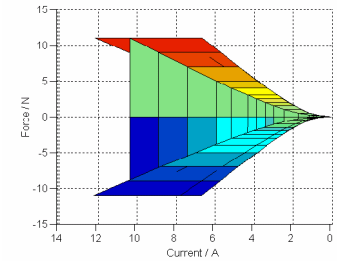

Fig. 26: Actual force against current in the proposed controller.

D. Simulation result

Before the motion test on the real prototype, the Matlab simulink software is applied to simulate the motor performance with different controllers. Assuming constant static friction and dynamic frictional gain, a long distance (100mm) and a short distance (250um) traveling simulations are done.

Both of position and velocity feedback gain (K_P, K_D) are kept constant in the experiments to ensure fair comparisons. For the long distance profile (i.e. 100mm), the position gain is 14200 and the velocity gain is 135. For the short distance profile (i.e. 250um), the position gain is 30000 and the velocity gain is 100.

1. Long distance (100mm)

For long distance (100mm) simulation, Fig. 27 shows that maximum dynamic error range is 0.35mm with the conventional controller. Appling the proposed controller, the error range is reduced to 0.16mm in Fig. 28. The improvement is around 54%. The maximum dynamic error is found at the highest acceleration and deceleration. The peak current and thus the greatest force are required accordingly.

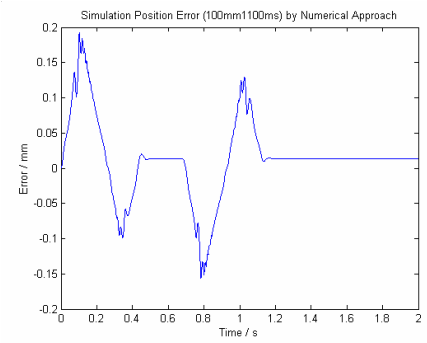

Fig. 27: Position error simulated by numerical approach on 100mm.

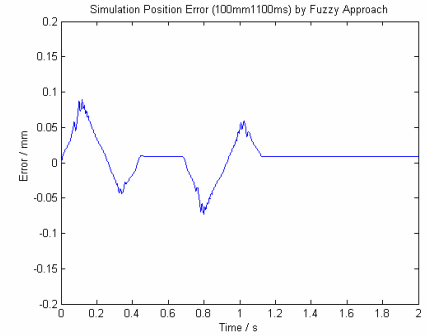

Fig. 28: Position error simulated by proposed controller on 100mm.

2. Short distance (250um)

For short distance (250um) simulation, the conventional controller is applied with the maximum dynamic error range 39um while the proposed controller reduces the error range to be 18um. The improvement is around 54%. The results are shown in Fig. 29 and Fig. 30. Similar to the long distance simulation result, the dynamic error, the exciting error and the force are found at the highest acceleration and deceleration.

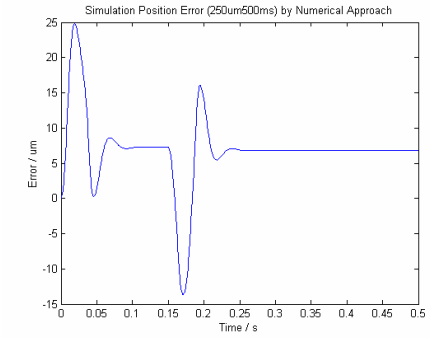

Fig. 29: Position error simulated by numerical approach on 250um.

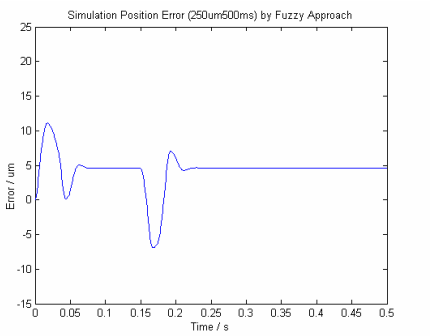

Fig. 30: Position error simulated by proposed controller on 250um.

From the simulation result above, the proposed controller is found to be better on the motion control of LSRM compared with the conventional numerical principle.

E. Experimental result

In real motor experiments, two traveling distances (100mm & 250um) are used as the default profiles to compare the performance between conventional and proposed controllers. For each profile, three experiments are taken.

The first test employs the numerical approach as the conventional controller. To verify the simulation result, the second experiment applies the fuzzy look-up table approach as the proposed controller. Finally, another fuzzy controller is implemented to replace the original PD controller.

For simplicity of motor control schemes,

A--- Numerical approach,

B--- Table look-up fuzzification with fixed PD control,

C--- Table look-up fuzzification with fuzzy PD control.

1. Long distance (100mm)

Motor control scheme	**Max. error range**	**Improve-ment**	**Compar-ison**
A	0.4mm	N/A	N/A
B	0.35mm	12.5%	Fig. 31
C	0.3mm	25%	Fig. 32

Table 3: Position accuracy summary of long distance (100mm) traveling.

Using fuzzy look-up approach, Fig. 31 shows that the maximum dynamic error is only 0.35mm and the accuracy is improved significantly by 12.5%. Since the force current distribution in LSRM is different from the typical permanent magnet motor, the special allocation loaded in look-up fuzzification table would solve the problem. Consequently, the controller becomes more intelligent and system can perform more efficiently.

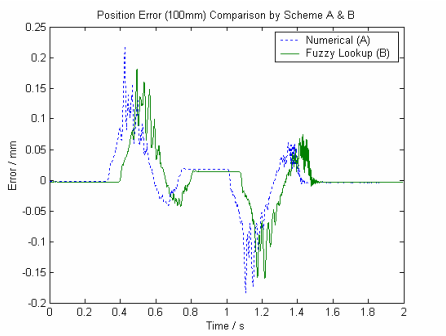

Fig. 31: Experimental position error by numerical and fuzzy approach on 100mm traveling.

After implementing two fuzzy controllers in the inner and outer loop, the maximum error is reduced from 0.4mm to 0.3mm with 25% accuracy improvement on 100mm profile. This significant improvement verifies the efficiency of fuzzy logic application in LSRM.

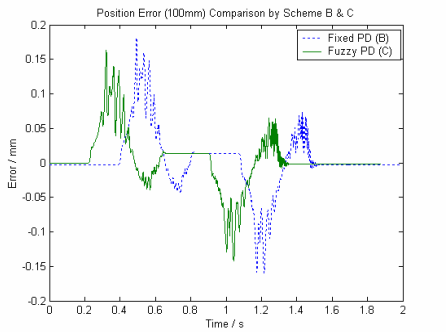

Fig. 32: Experimental position error by fixed PD and fuzzy logic supervising PD parameter approach on 100mm traveling.

2. Short distance (250um)

Motor control scheme	**Max. error range**	**Improve-ment**	**Compar-ison**
A	46um	N/A	N/A
B	41um	11%	Fig. 33
C	36um	21.7%	Fig. 34

Table 4: Position accuracy summary of short distance (250um) traveling.

Using fuzzy look-up approach on force current distribution control, the maximum dynamic error is only 41um and the accuracy is improved significantly by 11%.

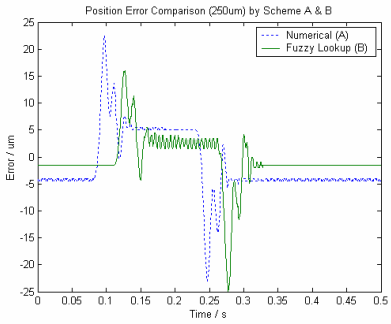

Fig. 33: Experimental position error by numerical and fuzzy approach on 250um traveling.

In the consequence, applying the proposed control method, fuzzy logic, in the inner and outer loop for 250um traveling distance, the maximum error is reduced from 46um to 36um. Such 21.7% improvement in motion control accuracy proves that the fuzzy logic controller provides much better performance on LSRM than the conventional numerical approach.

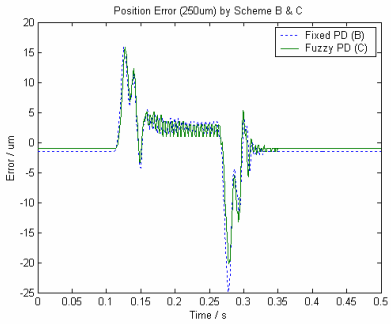

Fig. 34 : Experimental position error by fixed PD and fuzzy logic supervising PD parameter approach on 250um traveling.

Different from the permanent magnet motor, the LSRM has the magnetic flux nonlinear characteristics and cannot be expressed by numerical equations easily. In the conventional controller, the numerical equation expression is usually applied but finds difficulties. The look-up table fuzzification is proposed since it can well present such nonlinear characteristic in LSRM inner control loop. From the above experiments taken for long distance (100mm) and short distance (250um), the significant improvement proves the argument above.

The PD feedback controller is commonly used in control industry. However, the PD parameters have to be finely tuned for different traveling distances. In addition, this fine tuning procedure requires the knowledge and experience of control experts. Fuzzy PD supervising ability is very useful to save these experts manpower and allow general operators to handle some nonlinear systems. For the LSRM outer control loop, the PD fuzzy supervising is proposed. In two different motion profile tests, the experimental result highlights the advantages of fuzzy logic control and proves its efficiency.

V. CONCLUSIONS

In this research project, a robust LSRM system with a robust and reliable controller is developed. Applying switched reluctance technology, the conventional numerical controller always faces motion control problem due to magnetic flux nonlinearity. Shown by simulation and experimental results on different traveling distances, the proposed fuzzificed current force representation scheme is successful to provide an accurate and high efficiency controller on LSRM.

Beside the inner control loop regarding to exciting current and magnetic force, another fuzzy logic system supervising PD controller is proposed to reserve manpower on motion tuning. The significant position accuracy improvement strongly proves the extremely high robustness of the applied fuzzy controller.

VI. ACKNOWLEDGEMENT

The authors would like to thank the Hong Kong Polytechnic University for the funding of this research work through the Teaching Company Scheme Project Code: ZW82.

VII. REFERENCES

[1] T. J. E. Miller, *Switched Reluctance Motor and Their Control,* Magna Physics Publishing and Clarendon Press, Oxford, 1993.

[2] R. Krishnan, *Switched Reluctance Motor Drives: Modeling, Simulation, Analysis, Design, and Applications*, C.R.C. Press, 2001.

[3] R. C. Dorf and R. H. Bishop, *Modern Control Systems*, Addison Wesley, 1998.

[4] I. S. Shaw, *Fuzzy Control of Industrial Systems: Theory and Applications*, Kluwer Academic Publishers, 1998.

[5] L. X. Wang, *Adaptive Fuzzy Systems and Control: Design and Stability Analysis*, Prentice Hall PTR, 1994.

[6] B. S. Lee, H. K. Bae, P. Vijayraghavan and R. Krishnan, "Design of a linear switched reluctance machine," *IEEE Transactions on Industry Applications*, vol. 36, no. 6, pp.1571-1580, Nov., 2000.

[7] N. Matsui, N. Akao and T. Wakino, "High-precision torque control of reluctance motors", *IEEE Transactions on Industry Applications*, vol.27, no.5, Sep/Oct., 1991.

[8] S. C. P. Gomes and J. P. Chretien, "Dynamic modelling and friction compensated control of a robot manipulator joint," *IEEE International Conference on Robotics and Automation*, vol. 2, pp. 1429-1435, May, 1992.

[9] M. G.. Rodrigues, W. I. Suemitsu, P. Branco, J. A. Dente and L. G. B. Rolim, "Fuzzy logic control of a switched reluctance motor", *Proceedings of the IEEE International Symposium on Industrial Electronics*, vol. 2, pp. 527-531, Jul., 1997.

[10] A. E. Santo, M. R. A. Calado and C. M. P. Cabrita, "Long stroke linear switched reluctance actuator displacement with a fuzzy logic controller", *IEEE MELECON 2006*, pp. 1178-1181, May, 2006.

[11] H. Chen, J. Jiang, S. Sun and D. Zhang, "Dynamic simulation models of switched reluctance motor drivers", *IEEE Proceedings of the 3rd World Congress on Intelligent Control and Automation*, vol. 3, pp. 2111-2115, Jul., 2000.

[12] I. Husain, "Minimization of torque ripple in SRM drives", *IEEE Transactions on Industrial Electronics*, vol. 49, no. 1, pp. 28-39, Feb., 2002.

[13] L. X. Wang, *A Course in Fuzzy Systems and Control*, Prentice Hall PTR, 1997.

[14] H. Ying, *Fuzzy Control and Modeling: Analytical Foundations and Applications*, IEEE Press, 2000.

[15] N.C. Cheung, "A robust and low-cost linear motion system for precision manufacturing automation", *IEEE Industry Applications Conference*, vol. 1, pp. 40-45, Oct., 2000.

[16] N.C. Cheung, "A new type of direct-drive variable reluctance actuators for industrial automation", *IEEE International Conference on Industrial Technology*, vol. 1, pp. 30-34, 2002.

[17] W. C. Gan and N.C. Cheung, "Development and control of a low-cost linear variable-reluctance motor for precision manufacturing automation", *IEEE/ASME Transactions on Mechatronics*, vol. 8, no. 3, pp. 326-333, Sep., 2003.

[18] W.C. Gan, N.C. Cheung and L. Qiu, "Position control of linear switched reluctance motors for high-precision applications", *IEEE Transactions on Industry Applications*, vol. 39, no. 5, Sep., 2003.

[19] W.C. Gan, N.C. Cheung, "Design of a linear switched reluctance motor for high precision applications", *IEEE International Electric Machines and Drives Conference*, pp. 701-704, Jun., 2001.

[20] W.C. Gan, N.C. Cheung and L. Qiu, "Short distance position control for linear switched reluctance motors: a plug-in robust compensator approach", *Conference Record of the 2001 IEEE Industry Applications Conference. 36th IAS Annual Meeting*, vol. 4, pp. 2329-2336, Oct., 2001.